Human DDX3 protein is a valuable target to develop broad spectrum antiviral agents

Annalaura Brai[a], Roberta Fazi[a], Cristina Tintori[a], Claudio Zamperini[a], Francesca Bugli[b], Maurizio Sanguinetti[b], Egidio Stigliano[c], José Esté[d], Roger Badia[d], Sandra Franco[d], Miguel A. Martinez[d], Javier P. Martinez[e], Andreas Meyerhans[e,f], Francesco Saladini[g], Maurizio Zazzi[g], Anna Garbelli[h], Giovanni Maga[h,1], and Maurizio Botta[a,i,j,1]

[a]Dipartimento di Biotecnologie, Chimica e Farmacia, Università degli Studi di Siena, I-53100 Siena, Italy; [b]Istituto di Microbiologia, Università Cattolica del Sacro Cuore, 00168 Rome, Italy; [c]Institute of Pathological Anatomy, University Hospital A. Gemelli, Catholic University of Sacred Heart, 00168 Rome, Italy; [d]AIDS Research Institute, IrsiCaixa, Hospital Universitari Germans Trias i Pujol, Universitat Autònoma de Barcelona, 08916 Barcelona, Spain; [e]Infection Biology Group, Department of Experimental and Health Sciences, Universitat Pompeu Fabra, Parc de Recerca Biomedica Barcelona, 08003 Barcelona, Spain; [f]Institució Catalana de Recerca i Estudis Avançats, 08010 Barcelona, Spain; [g]Dipartimento di Biotecnologie Mediche, Università degli Studi di Siena, 53100 Siena, Italy; [h]Istituto di Genetica Molecolare, Consiglio Nazionale delle Ricerche (IGM-CNR), 27100 Pavia, Italy; [i]Sbarro Institute for Cancer Research and Molecular Medicine, Center for Biotechnology, College of Science and Technology, Temple University, Philadelphia, PA 19122; and [j]Lead Discovery Siena S.r.l., Castelnuovo Berardenga, 53019 Siena, Italy

Edited by Rino Rappuoli, GSK Vaccines, Siena, Italy, and approved March 23, 2016 (received for review November 20, 2015)

Targeting a host factor essential for the replication of different viruses but not for the cells offers a higher genetic barrier to the development of resistance, may simplify therapy regimens for coinfections, and facilitates management of emerging viral diseases. DEAD-box polypeptide 3 (DDX3) is a human host factor required for the replication of several DNA and RNA viruses, including some of the most challenging human pathogens currently circulating, such as HIV-1, Hepatitis C virus, Dengue virus, and West Nile virus. Herein, we showed for the first time, to our knowledge, that the inhibition of DDX3 by a small molecule could be successfully exploited for the development of a broad spectrum antiviral agent. In addition to the multiple antiviral activities, hit compound 16d retained full activity against drug-resistant HIV-1 strains in the absence of cellular toxicity. Pharmacokinetics and toxicity studies in rats confirmed a good safety profile and bioavailability of 16d. Thus, DDX3 is here validated as a valuable therapeutic target.

broad spectrum antivirals | DDX3 | host factors | resistance | coinfections

Most of the current therapeutic approaches to fight viral diseases target unique components or enzymes of a given virus with direct-acting antivirals. Although therapeutically highly successful, direct-acting antivirals are still suffering shortcomings, such as drug resistance, poor adherence in selected patient groups, and associated toxicity (1, 2). In addition, virtually no broad spectrum antivirals are currently available. An alternative approach currently exploited in antiviral research is the targeting of host proteins. Examples include Maraviroc (approved for the treatment of HIV-1 infection) and Alisporivir [in phase III trials for anti-Hepatitis C virus (HCV) therapy] (3, 4). Viruses as obligatory parasites dependent on the host cell machinery for replication, protein expression, and assembly of progeny particles (5–7). RNA viruses, in particular, have high mutation rates owing to their error-prone polymerases and rapidly generating drug-resistant variants (8–10). On this basis, blocking host cell factors required by different viruses for their replication might be a low cost and short time but effective route to develop broad spectrum antivirals able to limit the occurrence of drug resistance (11, 12).

Recent studies have revealed that the cellular ATPase/RNA helicase X-linked DEAD-box polypeptide 3 (DDX3) is an essential host factor for the replication of viruses belonging to different families: CMV (13) (*Herpesviridae*), HIV-1 (14) (*Retroviridae*), HCV (15–18), Japanese Encephalitis virus (19), Dengue virus (DENV) (20), West Nile virus (WNV; *Flaviviridae*) (21), Vaccinia virus (22–24) (*Poxviridae*), and Norovirus (25) (*Caliciviridae*). The exact mechanisms of interaction of this protein with individual pathogens are still poorly understood (26). Nonetheless, DDX3 is being regarded as an interesting target for the development of novel antiviral compounds (27, 28).

For example, targeting DDX3 might offer the possibility of simultaneously treating patients for HIV and HCV coinfections. Several inhibitors of the ATPase activity of DDX3 have been recently identified (29–34); however, an ATP-mimetic compound may have a low degree of selectivity in vivo because of the possibility of interacting with many targets (35).

Results and Discussion

In a recent work, we designed and validated the first small molecule DDX3 inhibitors, to our knowledge, specifically targeting its RNA binding site (Fig. 1) (36). The most promising molecule was compound **2**, with both antihelicase activity against DDX3 (IC_{50} = 1 μM) and inhibitory effects on HIV-1 replication in peripheral blood mononuclear cells [half-maximal effective concentration (EC_{50}) = 10 μM].

Pursuing this research line, a structure-based optimization process was prosecuted herein on compound **2**, resulting in the identification of a new family of more potent DDX3 inhibitors.

Because of the lack of a crystal structure of human DDX3 bound to RNA (closed conformation), we exploited an homology model previously built by us using the closed conformation of

Significance

Human DEAD-box polypeptide 3 (DDX3) is an ATPase/RNA helicase involved in the replication of many viral pathogens. We reported herein the first inhibitor, to our knowledge, of the helicase binding site of DDX3 endowed with a broad spectrum antiviral activity [HIV-1 WT, HIV drug-resistant strains, Hepatitis C virus (HCV), Dengue virus (DENV), and West Nile virus (WNV)]. The good toxicity profile suggests that the DDX3 activity, although essential for viruses, could be dispensable to the cells, validating DDX3 as a pharmaceutical target. Our results clearly showed that DDX3 inhibitors could be exploited to treat HIV/HCV coinfections, emerging infectious diseases (such as DENV and WNV), and HIV-1 patients carrying drug-resistant strains. Each of these three medical conditions currently represents a major challenge for clinical treatment.

Author contributions: G.M. and M.B. designed research; A.B., R.F., C.T., F.B., M.S., J.E., R.B., S.F., M.A.M., J.P.M., A.M., F.S., M.Z., and A.G. performed research; C.Z. and E.S. analyzed data; and A.B. wrote the paper.

The authors declare no conflict of interest.

This article is a PNAS Direct Submission.

Freely available online through the PNAS open access option.

[1]To whom correspondence may be addressed. Email: maga@igm.cnr.it or botta.maurizio@gmail.com.

This article contains supporting information online at www.pnas.org/lookup/suppl/doi:10.1073/pnas.1522987113/-/DCSupplemental.

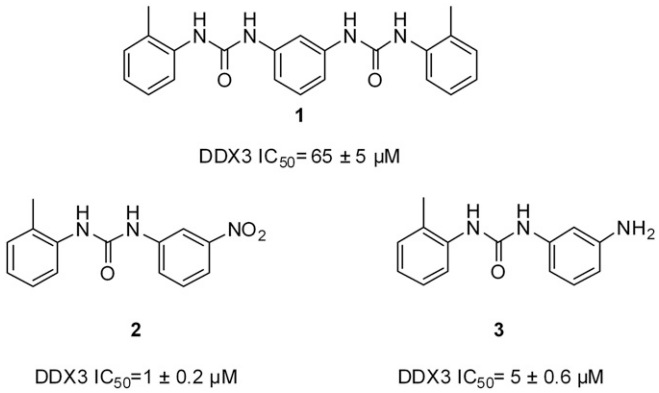

Fig. 1. 2D structures of the known human DDX3 inhibitors targeting the RNA binding pocket.

Drosophila Vasa DEAD-box helicase (Protein Data Bank ID code 2DB3) as a template (Fig. 2) (37).

Similar to the RNA strand (Fig. 2, yellow stick), compound **2** (Fig. 2, green stick) establishes important polar contacts with Arg276, Arg480, and Pro274. Furthermore, it makes hydrophobic interactions with Phe357, His472, Lys451, and Val500. However, our modeling analysis revealed the presence in the binding pocket of two unexplored areas that could be exploited in search of additional interactions (Fig. 2, cyan and magenta circles). Thus, a small library of compound **2** derivatives has been designed and synthesized, introducing modifications to probe these two regions and expand available structure–activity relationship (SAR) data. Slight modifications included the replacement of the nitro group with the isosteric carboxyl group and the substitution of the methyl–phenyl ring with a cyclohexyl moiety. Furthermore, a naphthyl ring was inserted in place of the tolyl terminus to make additional interactions with Arg503 and Val500. Next, more pronounced substitutions have been made by inserting a substituted triazole ring instead of the nitro group, which allowed the exploration of additional interactions involving residues Arg326 and Gly302. The para position was predicted by docking studies as the most appropriate for such

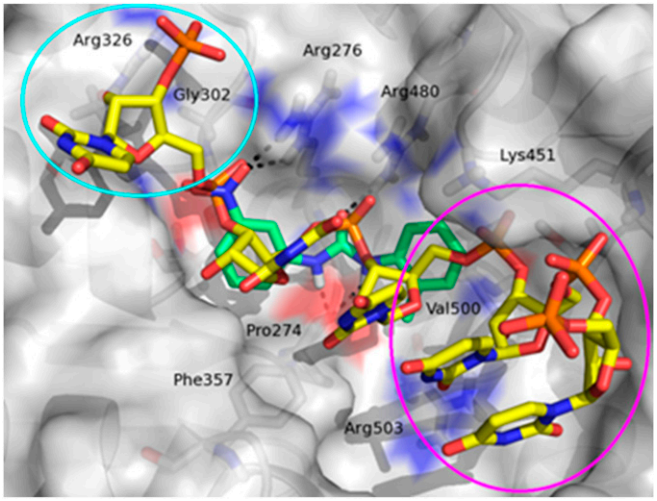

Fig. 2. Graphical representation of the DDX3 RNA binding site. The RNA strand is represented as yellow carbon sticks. The binding mode of compound **2** (green carbon sticks) was predicted by docking studies. Hydrogen bond interactions are visualized as black dashed lines. Compound **2** occupies a little part of the large pocket, and the two regions circled in magenta and cyan are unexplored by this ligand.

Table 1. DDX3 antienzymatic activity

Compound identification	Structure	IC_{50} (μM)
2	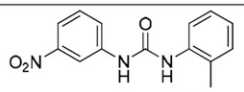	1
9	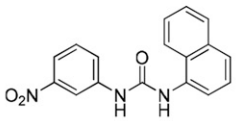	n.d*
10	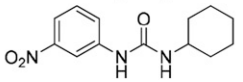	>200
11	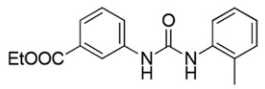	71.6
12	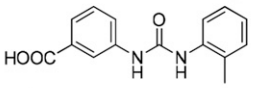	n.d*
16a	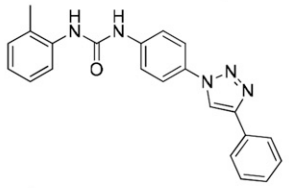	n.d*
16b	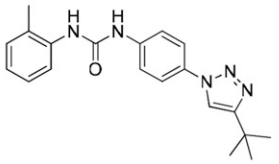	3.36
16c	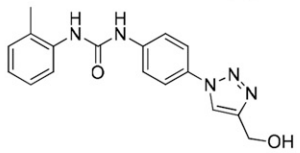	17.5
16d	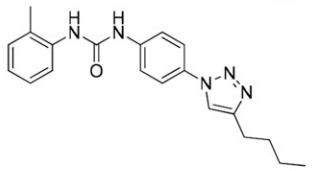	0.3
16e	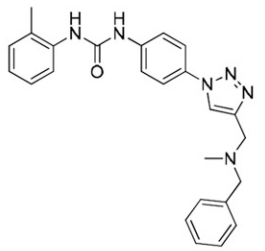	22.8
16f	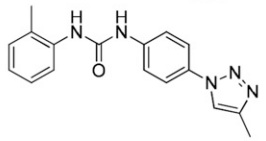	>100
16g	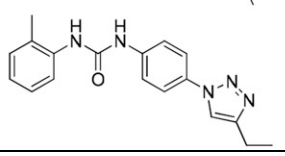	0.98

n.d., Not determined.
*Compound precipitated during assays.

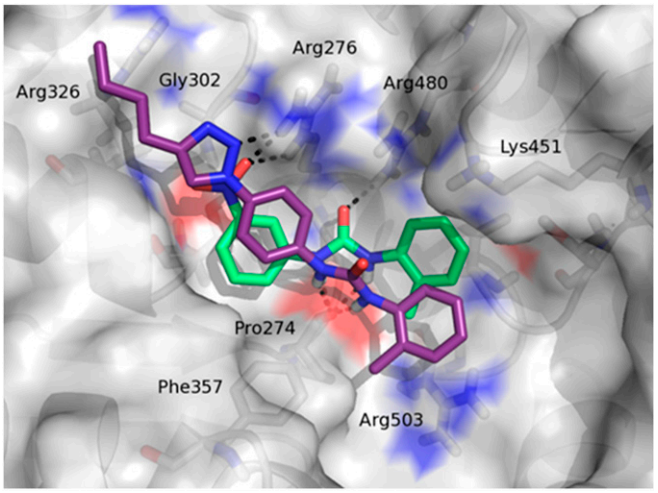

Fig. 3. Binding mode of compound **16d** (purple sticks). For comparison purpose, compound **2** (green sticks) was also visualized.

kinds of substitutions, and side chains at four positions were selected, taking into account the interactions into the pocket.

Synthesis of compounds **2**–**9** (Fig. S1) and **16a**–**16g** (Fig. S2) is reported in *Supporting Information*.

The anti-DDX3 activity of compounds was assayed, and results are shown in Table 1. Remarkably, the modifications aimed at optimizing the van der Waals contacts of the ligands with Arg276 and Arg326 (derivatives **16a**–**16g**) resulted in an increase of the helicase inhibitory activity, with the best inhibitors **16d** and **16g** having IC_{50} values of 0.3 and 0.98 μM, respectively.

The inactivity of compound **10** suggests that the presence of an aromatic moiety is fundamental for the helicase inhibitory activity, and is probably due to a crucial cation–π interaction with Arg503. Compounds **9** and **12** unexpectedly precipitated from medium in enzymatic assays and were, thus, found inactive, whereas the ester analog **11** was found moderately active.

The predicted binding mode of **16d** within the DDX3 RNA binding pocket is shown in Fig. 3. Some of the ligand contacts are coincident with the key interactions made by the parent compound **2**. Indeed, the urea NH groups were involved in hydrogen bonds with the backbone carbonyl oxygen of Pro274, whereas the triazole ring interacted with the guanidine group of Arg276. Moreover, the tolyl terminus established hydrophobic interactions with residues Arg503 and Pro274, and the phenyl ring made hydrophobic contacts with the aromatic side chain of Phe357. Finally, the butyl substituent at the four position of the triazole ring made profitable interactions with residues Arg326 and Gly302, was unexploited by compound **2**, and was probably responsible for the improved antihelicase activity.

According to the proposed mode of binding, **16d** behaved as a competitive inhibitor with respect to the RNA substrate, which

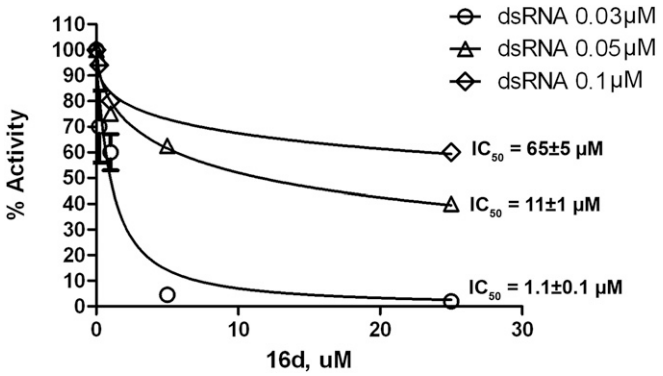

Fig. 4. Dose–response curves for DDX3 helicase activity inhibition by **16d** at increasing dsRNA substrate concentrations.

can be seen by the decrease in its inhibition potency as a function of increasing RNA substrate concentrations (Fig. 4).

The most active DDX3 inhibitor **16d** was then tested against HIV, HCV, WNV, and DENV. Results are summarized in Table 2. Remarkably, **16d** showed a broad spectrum of antiviral activity, being able to inhibit the replication of all of these viruses with EC_{50} values ranging from 0.97 to 16.5 μM. No toxicity was found in three different cell culture systems (LucUbiNeo-ET cells and Hepato cellular carcinoma cells) as a demonstration that the inhibition of a cellular cofactor essential for the viruses but not for the cells can represent a successful strategy for the development of novel antiviral agents. For comparison purpose, we also tested hit compound **2** that was previously published (36) against HCV-infected cells, but despite its activity against DDX3, it was found inactive (EC_{50} > 86 μM).

The NS3 protein of both HCV and DENV is an RNA helicase that belongs to the same family of DDX3. To exclude the involvement of such viral enzymes in the activities of **16d**, we tested this compound against NS3 proteins of HCV and DENV as well as against another cellular member of the DEAD-box family, namely DDX1. We also tested the ability of **16d** in the inhibition of the ATPase activity of DDX3. As shown in Table 3, **16d** was found to be completely inactive against the ATPase of DDX3, DDX1 helicase, and DENV NS3 helicase. It showed moderate activity against the HCV NS3 helicase, which was, however, 56- and 17-fold lower than the activity against DDX3 helicase and HCV proliferation, respectively.

The antiviral activity of compound **16d** was also evaluated against HIV-1 strains carrying clinically relevant mutations conferring high-level resistance to most classes of antivirals approved to treat HIV infection (Table 4 and Table S1). Compound **16d** retained full activity against all of the resistant viruses tested, confirming its novel mechanism of action and the potential to overcome HIV resistance.

A few in vitro experiments were then conducted to quickly establish the absorption/stability of compound **16d**: aqueous solubility (pH 7.4 buffer), parallel artificial membrane permeability

Table 2. Antiviral activities

Virus	Strain	Cell type	EC_{50} **16d** (μM)	CC_{50} **16d** (μM)	EC_{50} **10** (μM)	CC_{50} **10** (μM)	EC_{50} **16f** (μM)	CC_{50} **16f** (μM)
HIV*	NL4-3	PBMCs	1.1	>200	110	>200	>50	50
HCV†	Replicon	LucUbiNeo-ET	0.97	49.77	>80	80	>36	36
DENV‡	2, New Guinea C	Huh7	2.55	>200	nt	nt	nt	nt
WNV‡	NY99	Huh7	16.5	>200	nt	nt	nt	nt

CC_{50}, half-maximal cytotoxic concentration; EC_{50}, half-maximal effective concentration; nt, Not tested; PBMC, peripheral blood mononuclear cell.
*Evaluated in PBMCs.
†Evaluated in LUNET:LucUbiNeo-ET cells.
‡Evaluated in Huh7:Hepato cellular carcinoma cells.

Table 3. Enzymatic data on compound 16d

ATPase DDX3 IC_{50} (μM)	DDX1 IC_{50} (μM)	NS3 (DENV) IC_{50} (μM)	NS3 (HCV) IC_{50} (μM)
>200*	>200	>200	16.8

*The value >200 indicates that less than 20% of inhibition was observed at 200 μM, the highest concentration that was tested.

assay, and human liver microsome stability determination (Table 5). Despite the fact that the aqueous solubility is just outside of the range of recommended values for a drug ($-6 <$ LogS < -1), the excellent metabolic stability and the good passive membrane permeability make **16d** a good lead candidate for additional development.

Table 4. Antiviral activity of compound 16d against HIV-1 strains carrying the most common patterns of resistance mutations selected by drugs currently used to treat HIV-1 infection

HIV-1 strain*	Drug resistance class	IC_{50} (95% confidence interval; μM)	Fold change†
114‡	WT	1.11 (0.31–3.90)	—
11808	PIs	0.23 (0.08–0.65)	0.2
7406	NRTIs	0.33 (0.13–0.87)	0.3
7404	NRTIs	0.22 (0.11–0.47)	0.2
12227	NNRTIs	0.94 (0.21–1.34)	0.8
12235	NNRTIs	0.36 (0.15–0.87)	0.3
11845	INIs	0.37 (0.26–0.52)	0.3

INI, integrase inhibitor; NNRTI, nonnucleoside reverse transcriptase inhibitor; NRTI, nucleoside reverse transcriptase inhibitor; PI, protease inhibitor. —, no fold change.
*NIH AIDS Reagent Program catalog number (https://www.aidsreagent.org).
†Resistant strain IC_{50} to WT strain IC_{50} ratio.
‡NL4-3 HIV-1 WT reference strain.

Table 5. 16d in vitro absorption, distribution, metabolism, and excretion (ADME) studies

Papp*	Membrane retention†	LogS‡	HLM stability§
$2.86 \cdot 10^{-6}$	19.1	−7.05	99

HLM, human liver microsome; Papp, apparent permeability.
*Papp reported in centimeters·seconds^{-1}.
†Membrane retention expressed as percentage.
‡Aqueous solubility.
§HLM metabolic stability expressed as percentage of unmodified parent drug.

To better evaluate toxicity and biodistribution of compound **16d**, we finally performed several preliminary in vivo studies; **16d** was administered to Wistar rats by tail vein in a single systemic dose (0.05 mL per dose) at high-dose levels of 20 mg/kg. There were no treatment-related adverse effects on clinical chemistry analysis of serum for the measurement of biochemical parameters (including liver enzymes, such as alanine aminotransferase, aspartate aminotransferase, and glutamate dehydrogenase), urea, creatinine, triglycerides, LDLs, and HDLs. Urine analysis parameters for treated rats did not show any significant difference from the respective control groups. Histopathological analysis

Table 6. Pharmacokinetic parameters of 16d after i.v. administration at a dose of 10 mg·kg^{-1}

Pharmacokinetic parameters	16d*
Dose (mg/kg)	10.00
MRT (h)	3.98 ± 0.38
$AUC_{0-\infty}$ (μg × h/mL)	39.95 ± 13.50
AUC_{0-24} (μg × h/mL)	39.77 ± 13.51
CL (mL/min)	1.29 ± 0.54
$t_{1/2\beta}$ (h)	3.19 ± 0.24

AUC, area under the plasma concentration–time curve; CL, plasma clearance; MRT, mean residence time; $t_{1/2\beta}$, plasma half-life.
*All data are expressed as means ± SDs ($n = 3$).

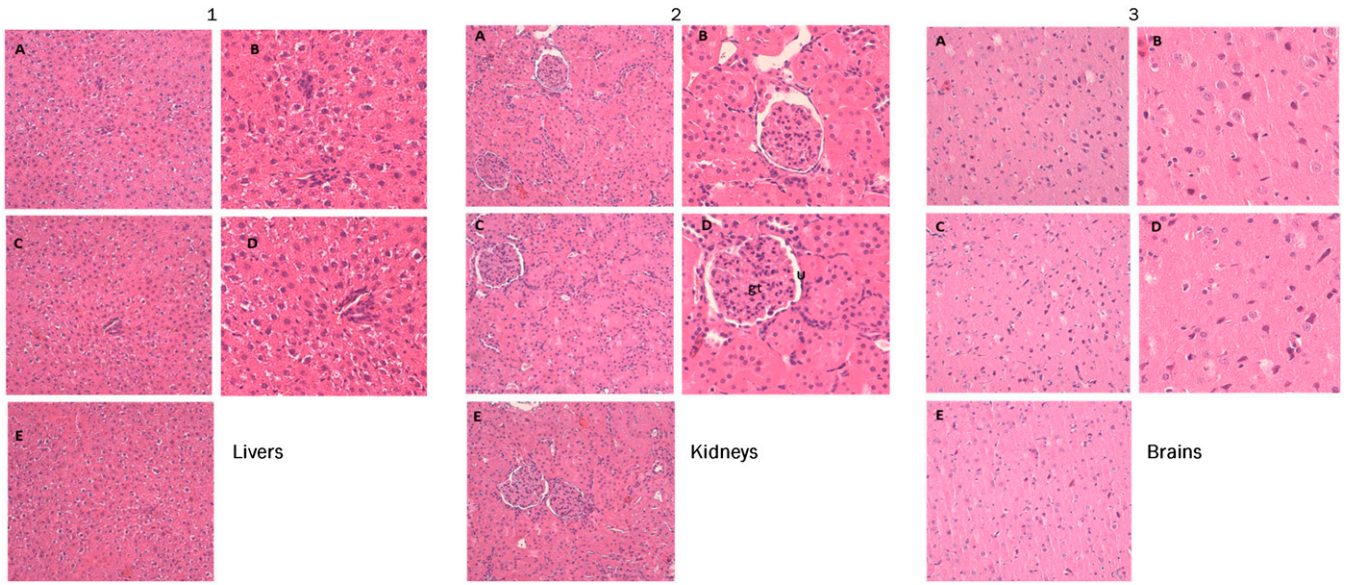

Fig. 5. Representative images of the histological examination of H&E-stained sections of (*A1–E1*) livers, (*A2–E2*) kidneys, and (*A3–E3*) brains from three groups of rats. (*A1–A3* and *B1–B3*) VG. (*C1–C3* and *D1–D3*) TG. (*E1–E3*) WT group. Treated rats do not exhibit abnormal histopathological changes compared with the control group. The microphotographs were taken using a digital camera (Nikon SLR-D3000) at original magnifications of 100× and 200×. gt, Glomerular tuft; U, urinary space.

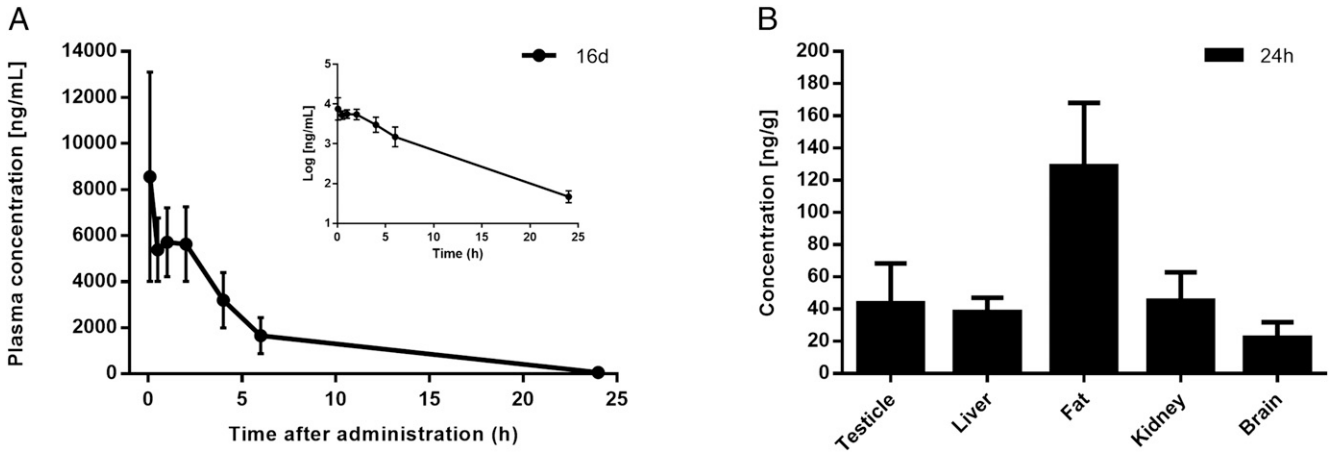

Fig. 6. Pharmacokinetic parameters and tissue distribution in rats; **16d** was administered as a single i.v. bolus injection of 10 mg/kg per group ($n = 3$). Data points represent the means ± SDs. (*A*) Plasma level curves of **16d**. The semilogarithmic plot is shown in *Inset*. The elimination curve showed a first-order kinetic that showed an exponential decrease in the semilogarithmic plot. (*B*) Concentration levels of **16d** in rat tissues at 24 h after single-dose administration.

of the liver was free from any pathological abnormality, and H&E-stained sections appeared normal, with regular cellular architecture. The hepatic cells had intact cytoplasm, sinusoidal spaces, prominent nucleus, and nucleolus (Fig. 5). Renal tissue of all animal groups showed preserved renal parenchyma with normal appearance of glomerular tuft and urinary space (Fig. 5). Also, histological analyses of brain tissue samples showed no obvious uncharacteristic changes in all animal groups. In conclusion, **16d** was found to possess excellent biocompatibility, and Wistar rats showed a good tolerance to the dose of 20 mg/kg.

The pharmacokinetic analysis of compound **16d** was finally conducted. The main pharmacokinetic parameters from single-compartment model analysis are summarized in Table 6. The half-life elimination and the plasmatic clearance values denoted that **16d** was rapidly eliminated after i.v. administration.

The mean plasma concentration–time curves after i.v. administration are illustrated in Fig. 6*A*. Tissue distribution of **16d** in rat after i.v. administration is presented in Fig. 6*B*. Higher concentration of **16d** was found in adipose tissue followed by kidney, testicle, liver, and brain in that order, which can be attributed to the blood flow in this organs.

In conclusion, we report herein the discovery of a novel series of human helicase DDX3 inhibitors. Among them, compound **16d** represents the first compound, to our knowledge, achieving broad spectrum antiviral activity (HIV, HCV, DENV, and WNV) in infected cells, targeting a host factor. Compound **16d** was active against HIV-1 drug-resistant strains, suggesting that DDX3 targeting agents may be able to treat HIV/HCV coinfections, patients harboring drug-resistant viruses, and emerging viral diseases, for which no specific drugs are available. Moreover, the good toxicity profile suggests that the DDX3 activity, although essential for viral replication, may be dispensable to the cell as shown by preclinical studies. This result represents a step forward in the fight against infectious diseases and opens a new scenario in the drug development process.

Materials and Methods

Detailed procedures for the synthesis and characterization of compounds are provided in *Supporting Information*.

Absorption, distribution, metabolism, and excretion (ADME) experiments, assay protocols, and pharmacokinetic and toxicity studies can be found in *Supporting Information*.

The rat experiments were performed under a protocol approved by the Institutional Animal Use and Care Committee at the Università Cattolica del Sacro Cuore (permit no. EE21; March 18, 2014) and authorized by the Italian Ministry of Health according to the Legislative Decree 116/92, which implemented the European Directive 86/609/EEC on laboratory animal protection in Italy. Animal welfare was routinely checked by veterinarians of the Service for Animal Welfare.

ACKNOWLEDGMENTS. The authors gratefully acknowledge use of the facilities provided by Lead Discovery Siena S.r.l. in collaboration with First Health Pharmaceuticals B.V. of Amsterdam. This research was supported by First Health Pharmaceuticals B.V., Tuscany Region Grant DD3242/2009 Bando Salute 2009, and Prin 2010 Research Project Grant 2010W2KM5L. This work was also supported by Spanish Ministry of Economy and Competitiveness (MINECO) Fondo Europeo de Desarrollo Regional (FEDER) Grants SAF2013-46077-R and BFU2015-63800R.

1. Lou Z, Sun Y, Rao Z (2014) Current progress in antiviral strategies. *Trends Pharmacol Sci* 35(2):86–102.
2. Bekerman E, Einav S (2015) Infectious disease. Combating emerging viral threats. *Science* 348(6232):282–283.
3. Dorr P, et al. (2005) Maraviroc (UK-427,857), a potent, orally bioavailable, and selective small-molecule inhibitor of chemokine receptor CCR5 with broad-spectrum anti-human immunodeficiency virus type 1 activity. *Antimicrob Agents Chemother* 49(11):4721–4732.
4. Gallay PA, Lin K (2013) Profile of alisporivir and its potential in the treatment of hepatitis C. *Drug Des Devel Ther* 7:105–115.
5. Ahlquist P, Noueiry AO, Lee WM, Kushner DB, Dye BT (2003) Host factors in positive-strand RNA virus genome replication. *J Virol* 77(15):8181–8186.
6. Prussia A, Thepchatri P, Snyder JP, Plemper RK (2011) Systematic approaches towards the development of host-directed antiviral therapeutics. *Int J Mol Sci* 12(6): 4027–4052.
7. Scheller N, et al. (2009) Translation and replication of hepatitis C virus genomic RNA depends on ancient cellular proteins that control mRNA fates. *Proc Natl Acad Sci USA* 106(32):13517–13522.
8. Drake JW, Holland JJ (1999) Mutation rates among RNA viruses. *Proc Natl Acad Sci USA* 96(24):13910–13913.
9. Gianella S, Richman DD (2010) Minority variants of drug-resistant HIV. *J Infect Dis* 202(5):657–666.
10. Duffy S, Shackelton LA, Holmes EC (2008) Rates of evolutionary change in viruses: Patterns and determinants. *Nat Rev Genet* 9(4):267–276.
11. Ruiz A, Russell SJ (2012) A new paradigm in viral resistance. *Cell Res* 22(11):1515–1517.
12. Martinez JP, Sasse F, Brönstrup M, Diez J, Meyerhans A (2015) Antiviral drug discovery: Broad-spectrum drugs from nature. *Nat Prod Rep* 32(1):29–48.
13. Lenarcic EM, Ziehr BJ, Moorman NJ (2015) An unbiased proteomics approach to identify human cytomegalovirus RNA-associated proteins. *Virology* 481:13–23.
14. Yedavalli VS, Neuveut C, Chi YH, Kleiman L, Jeang KT (2004) Requirement of DDX3 DEAD box RNA helicase for HIV-1 Rev-RRE export function. *Cell* 119(3):381–392.
15. Owsianka AM, Patel AH (1999) Hepatitis C virus core protein interacts with a human DEAD box protein DDX3. *Virology* 257(2):330–340.
16. Mamiya N, Worman HJ (1999) Hepatitis C virus core protein binds to a DEAD box RNA helicase. *J Biol Chem* 274(22):15751–15756.
17. You LR, et al. (1999) Hepatitis C virus core protein interacts with cellular putative RNA helicase. *J Virol* 73(4):2841–2853.
18. Ariumi Y, et al. (2007) DDX3 DEAD-box RNA helicase is required for hepatitis C virus RNA replication. *J Virol* 81(24):13922–13926.
19. Li C, et al. (2014) Cellular DDX3 regulates Japanese encephalitis virus replication by interacting with viral un-translated regions. *Virology* 449:70–81.

20. Noble CG, et al. (2010) Strategies for development of Dengue virus inhibitors. *Antiviral Res* 85(3):450–462.
21. Chahar HS, Chen S, Manjunath N (2013) P-body components LSM1, GW182, DDX3, DDX6 and XRN1 are recruited to WNV replication sites and positively regulate viral replication. *Virology* 436(1):1–7.
22. Schröder M, Baran M, Bowie AG (2008) Viral targeting of DEAD box protein 3 reveals its role in TBK1/IKKepsilon-mediated IRF activation. *EMBO J* 27(15):2147–2157.
23. Kalverda AP, et al. (2009) Poxvirus K7 protein adopts a Bcl-2 fold: Biochemical mapping of its interactions with human DEAD box RNA helicase DDX3. *J Mol Biol* 385(3): 843–853.
24. Benfield CT, Ren H, Lucas SJ, Bahsoun B, Smith GL (2013) Vaccinia virus protein K7 is a virulence factor that alters the acute immune response to infection. *J Gen Virol* 94(Pt 7): 1647–1657.
25. Vashist S, Urena L, Chaudhry Y, Goodfellow I (2012) Identification of RNA-protein interaction networks involved in the norovirus life cycle. *J Virol* 86(22):11977–11990.
26. Schröder M (2011) Viruses and the human DEAD-box helicase DDX3: Inhibition or exploitation? *Biochem Soc Trans* 39(2):679–683.
27. Tintori C, et al. (2014) Protein-protein interactions and human cellular cofactors as new targets for HIV therapy. *Curr Opin Pharmacol* 18:1–8.
28. Dürr R, et al. (2014) Targeting cellular cofactors in HIV therapy. *Topics in Medicinal Chemistry*, eds Diederich WE, Steuber H (Springer, Heidelberg), pp 183–222.
29. Yedavalli VS, et al. (2008) Ring expanded nucleoside analogues inhibit RNA helicase and intracellular human immunodeficiency virus type 1 replication. *J Med Chem* 51(16):5043–5051.
30. Zhang N, Zhang P, Baier A, Cova L, Hosmane RS (2014) Dual inhibition of HCV and HIV by ring-expanded nucleosides containing the 5:7-fused imidazo[4,5-e][1,3]diazepine ring system. In vitro results and implications. *Bioorg Med Chem Lett* 24(4):1154–1157.
31. Garbelli A, et al. (2011) Targeting the human DEAD-box polypeptide 3 (DDX3) RNA helicase as a novel strategy to inhibit viral replication. *Curr Med Chem* 18(20):3015–3027.
32. Maga G, et al. (2008) Pharmacophore modeling and molecular docking led to the discovery of inhibitors of human immunodeficiency virus-1 replication targeting the human cellular aspartic acid-glutamic acid-alanine-aspartic acid box polypeptide 3. *J Med Chem* 51(21):6635–6638.
33. Samal SK, Routray S, Veeramachaneni GK, Dash R, Botlagunta M (2015) Ketorolac salt is a newly discovered DDX3 inhibitor to treat oral cancer. *Sci Rep* 5:9982.
34. Bol GM, et al. (2015) Targeting DDX3 with a small molecule inhibitor for lung cancer therapy. *EMBO Mol Med* 7(5):648–669.
35. Bantscheff M, Scholten A, Heck AJ (2009) Revealing promiscuous drug-target interactions by chemical proteomics. *Drug Discov Today* 14(21-22):1021–1029.
36. Radi M, et al. (2012) Discovery of the first small molecule inhibitor of human DDX3 specifically designed to target the RNA binding site: Towards the next generation HIV-1 inhibitors. *Bioorg Med Chem Lett* 22(5):2094–2098.
37. Fazi R, et al. (2015) Homology model-based virtual screening for the identification of human helicase DDX3 inhibitors. *J Chem Inf Model* 55(11):2443–2454.
38. Verdonk ML, Cole JC, Hartshorn MJ, Murray CW, Taylor RD (2003) Improved protein-ligand docking using GOLD. *Proteins* 52(4):609–623.
39. Cole JC, Nissink JWM, Taylor R (2005) Protein-ligand docking and virtual screening with GOLD. *Virtual Screening in Drug Discovery*, eds Shoichet B, Alvarez J (Taylor & Francis CRC Press, Boca Raton, FL).
40. PyMOL (2011) *PyMOL Molecular Graphics System, Version 0.99* (Schrödinger, LLC, New York, NY).
41. Pannecouque C, Daelemans D, De Clercq E (2008) Tetrazolium-based colorimetric assay for the detection of HIV replication inhibitors: Revisited 20 years later. *Nat Protoc* 3(3):427–434.
42. Wohnsland F, Faller B (2001) High-throughput permeability pH profile and high-throughput alkane/water log P with artificial membranes. *J Med Chem* 44(6): 923–930.
43. Sugano K, et al. (2001) High throughput prediction of oral absorption: Improvement of the composition of the lipid solution used in parallel artificial membrane permeation assay. *J Biomol Screen* 6(3):189–196.
44. Shumaker RC (1986) PKCALC: A BASIC interactive computer program for statistical and pharmacokinetic analysis of data. *Drug Metab Rev* 17(3-4):331–348.